

Effect of polymeric-metallic synthesized Fe₃O₄ Nano-carrier for bleomycin drug on AKT1 gene expression and cytotoxicity in renal cancer therapy

Samar Nahrawan

*Faculty of Biotechnology, Al-Qasim Green University, Babylon, Iraq,
samar.n@biotech.uoqasim.edu.iq*

Salih Abdul-Mahdi

*Faculty of Biotechnology, Al-Qasim Green University, Babylon, Iraq,
s70217313@gmail.com*

Abstract

Herein, a drug delivery Nano-carrier was composed of a dextran (DEX) coated superparamagnetic iron nanoparticles (SPIONs) and decorated with folate (FA) to encapsulate bleomycin (BLN). These Nano-formulations in the present project were utilized in vitro to treat kidney cancer cells with anticancer agents. Vibrating sample magnetometer (VSM), X-ray diffraction (XRD), electron microscopy (TEM), Fourier transform infrared spectroscopy (FTIR), and scanning electron microscopy (SEM), dynamic light scattering (DLS). drug encapsulation, and drug release profile were used to characterize the obtained SPION-DEX-BLN-FA in terms of its structural, magnetic, morphological, and size properties. By employing methyl thiazolyl tetrazolium, the effect of SPION-DEX-BLN-cellular FA's toxicity and its ability to induce apoptosis were assessed (MTT) additional to Real Time-PCR tests on kidney cancer A-498 and healthy HK-2 cell lines. The results revealed that the generated NPs were spherical, had acceptable dispersion, and without any agglomeration. The NPs' sizes bare was 29 ± 7.7 whereas the size of all (SPION-DEX-BLN-FA) was 72 ± 23 . Present study showed that SPION-DEX-BLN-FA demonstrated significant cell cytotoxicity induction, on A-498 cells. the present findings demonstrated that SPION-DEX-FA employ synergistic effects to target BLN delivery intracellularly, and in contrast to untreated control cells, the levels of mRNA AKT1 gene was lower gene expression the fold change mean was 0.452 ± 0.08 when treated with SPION-DEX-BLN-FA whereas fold change mean was 1.318 ± 0.05 with SPION-DEX-FA (bare BLN).

Keywords: *SPION, Bleomycin, AKT1, kidney cancer.*

1. INTRODUCTION

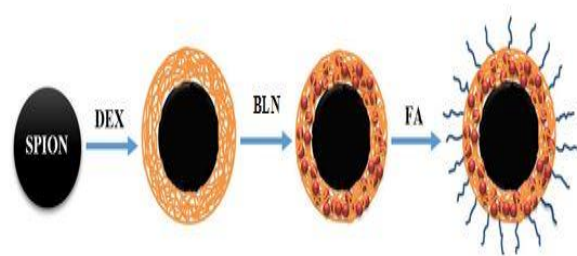
In addition to other malignancies such testicular, ovarian, cervical, renal, and liver cancers, the chemotherapeutic drug bleomycin (BLN) is widely used to treat kidney cancer. Bleomycin triggers cancer cell death via its capacity to generate radical oxygen species (ROS). Moreover, the concentrations of bleomycin in tumors have not yet been

determined. One of the most popular anti-cancer medications is the agent BLN, however there are certain negative effects. This limits its applicability in clinical settings (1,2). Serine/threonine protein kinase AKT1, commonly referred to as AKT kinase, controls a number of signaling downstream pathways that are involved in cell metabolism, proliferation, survival, growth, and angiogenesis (3). One of the most frequently

active protein kinases in malignancies of humans is AKT. AKT hyper-activation may encourage cell development, promote cell proliferation, and help cells avoid apoptosis. (4,5,6,7)

For biological applications such as targeted drug delivery, magnetic particle imaging (MPI), magnetic fluid hyperthermia (MFH), and separation of biomolecules, superparamagnetic iron oxide nanoparticles (SPION) are frequently utilized (8,9). The current study's findings were attained using a dual targeted SPION-DEX-BLN-FA synthesis and an active carrier framework design. (shown in Figure 1), In this study, the SPIONs are viewed as a Nano-carrier core for enhancing targeted delivery of BLN into kidney cancer cell lines because they include a chemotherapeutic agent. (10,11). Herein, the SPION was coated by dextran (DEX) and decorated with folate (FA) to encapsulate bleomycin (BLN) for treating the kidney cancer cell lines. Morphological characterizations, structural, size, magnetic, and drug loading activities of the obtained SPION-DEX-BLN-FA were performed by FTIR, XRD, VSM, SEM, TEM, drug encapsulation and drug release profile. Cellular toxicity effect of SPION-DEX-BLN-FA was evaluated by using of methyl thiazolyl tetrazolium (MTT), and real time PCR tests on kidney cancer A-498 and healthy HK-2 cell lines.

Figure 1. Schematically shown the steps of synthesizing and producing of SPION@DEX-BLN-FA NPs.



2. Materials and methods

2.1 Materials

The Merck company provided all the materials for this project, including the BLN medication, DEX, DMSO, FeCl₃6H₂O, FeCl₂4H₂O, MTT powder, NH₄OH, and Folate. Both healthy (HK-2) and kidney cancer (A-498) cell lines were bought from ATCC, USA. The remaining supplies were bought from Sigma Aldrich, USA.

2.2 SPION Preparation

The co-precipitation method, which was selected to preparing of SPION as a carrier of BLN in this work according to previous methods for the same purpose. (12,13).

2.3 Preparation of SPION-DEX-BLN-FA

Preparation procedure achieved according to Albukhaty in 2020 and Levy 2004. Briefly, 2.0 mg of dextran powder was added to 250 ml of deionized water, then 100 mg of BLN previously dissolved in 5 mL of deionized water). The concentration of BLN unloaded was measured in the supernatant (13,14). Equation (1) was used to determine the efficacy of drug encapsulation:

$$\text{Encapsulation efficiency (\%)} = \frac{[(\text{drug fed} - \text{drug loss}) / (\text{drug fed})] \times 100\%}{\text{Eq. 1}}$$

2.4. Characterization of the synthesized Nano-formulation

2.4.1. Size, charge, polydispersity and morphological characteristics of prepared NPs

Dynamic light scattering using Zeta potential analyzer (MALVERN, Nano S, UK) was employed to evaluate the average diameter size, charge and, polydispersity of SPION and SPION-DEX-BLN-FA. TEM, DLS and SEM were used to determine the morphological properties of prepared NPs that used in present study.

2.4.2. Fourier transform infrared (FT-IR)

The functional groups on the surface of the artificial Nano-formulation for pure polymer, coated and non-coated nanoparticles were studied by using of FT-IR spectrometer (Matson1000, Unican, USA) and KBr pellets in the 400–4000 cm⁻¹ range.

2.4.3. X-ray diffraction (XRD) and vibrating sample magnetometer (VSM)

utilizing the X-ray diffractometer (Bruker D8) and Cu K radiation system (= 0.1540 nm) (Germany), SPIONs' crystal structure and phase analysis were investigated. Diffraction patterns were acquired at an accelerating voltage of 40 kV with diffraction angles between 2θ= 5-70°. For data analysis, the software PAN-Alytical X'pert high score was used. magnetic characteristics of SPION, Fe₃O₄@DEX, Fe₃O₄@DEX-BLN, Fe₃O₄@DEX-BLN-FA. The magnetometer (VSM, Lakeshore 7404, USA) was used to analyze a vibrating sample.

2.5. Measurement of drug release

Phosphate-buffered saline and citrate buffer (0.01 M, pH = 7.4 and 0.01 M, pH = 5.4 respectively) at 37 °C were used separately to achieve BLN drug release from SPION@DEX-FA. Each of these buffer solutions has Tween 80 added as an emulsifying reagent to avoid any potential drug release sedimentation. At 0, 4, 8, 12, 24, 48, 72, and 96 hours, sampling was carried out. 500 μL of the specimen were obtained at each time point and subjected to freeze-drying process. Following equation was used to calculate the drug's release (13,14).

$$R = \frac{V \sum_{i=1}^{n-1} C_i + V_0 C_n}{m_{drug}} \quad \text{Eq. 2}$$

Releasing of drug (percent), represented by R, while the volume of sampling indexed by V, V₀ represent the initial drug volume, C_i, C_n are the drug concentration, “i” represented the

testing moment, “n”, and "mdrug" is the drug mass in the nanocarrier. Once more double-distilled water was used to wash the sediment substance.

2.6 Condition of Cell Culture

A-498 kidney cancer and HK-2 healthy cell lines were grown in the Gibco, Life Technologies (UK and Plymouth, MN, USA) growth medium (DMEM) supplemented with 10% fetal bovine serum (FBS) in addition to penicillin/streptomycin at 37°C in a humidified incubator with 5% CO₂.

2.7 Methyl thiazolyl tetrazolium (MTT) assay

The outcomes of the MTT experiment used to examine the cytotoxicity of SPIONs against the Both healthy (HK-2) and kidney cancer (A-498) cell lines. Procedure achieved according to Albukhaty in 2020 and Levy 2004. Briefly A 200 μl medium containing 1x 10⁴ cells were added to each well to fulfill the MTT assay. By using of a multi-scan plate reader, the absorbance of each well was measured at 540 nm (Versa Max Microplate Reader, Molecular Device, CA, USA). In order to get the results, mean and SD were used.

$$\text{Relative cell toxicity} = \left[\frac{(A_{\text{sample}} - A_{\text{control}})}{A_{\text{control}}} \right] \times 100 \quad \text{Eq. (3)}$$

2.8 Real Time-PCR

After 48 hours of treatment with SPION-DEX-BLN-FA, void BLN drug, and bare nano-carrier SPION-DEX-FA, the total RNA was extracted from was extracted from cultured cells by using of Invitrogen TRIzo reagent (UK). To determine the concentration of RNA, the optical density at 260/280 wavelength was used. We used cDNA synthesis ((Fermentas, Germany) to produce cDNA from the whole RNA. Reverse and forward primers for the Actin, BAX, and Akt-1 genes were created and used in this study, as shown in Table. Five pairs of primers for

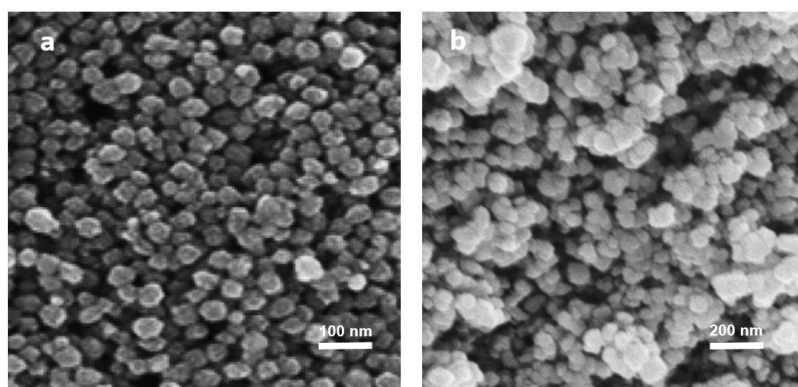
targets and endogenous gen included the temperature, duration, and cycles number for each step were utilize and referenced (16-17) in accordance with the kit's manufacturer's recommendations.

3. Result

3.1. Characterization of synthesized nanoparticles

3.1.1. Microscopic analysis

Figure 2. SEM image of SPION (a) and SPION@DEX-BLN-FA (b).



3.1.2. Size, Charge and Polydispersity

Size and polydispersity of SPION in 25 °C was 29 ± 41 nm and 0.055 nm, respectively (figure 3 a). On the another hand, the figure 4 a shows

that the size and polydispersity of SPION-DEX-BLN-FA in 25 °C was 72 ± 23 nm and 0.074 nm, respectively. Figure 3 b and figure 4 b indicated respectively the charge of SPION (-19.8) and SPION-DEX-BLN-FA (-33.8).

Figure 3. size (a) and charge (b) of SPION using dynamic light scattering (DLS).

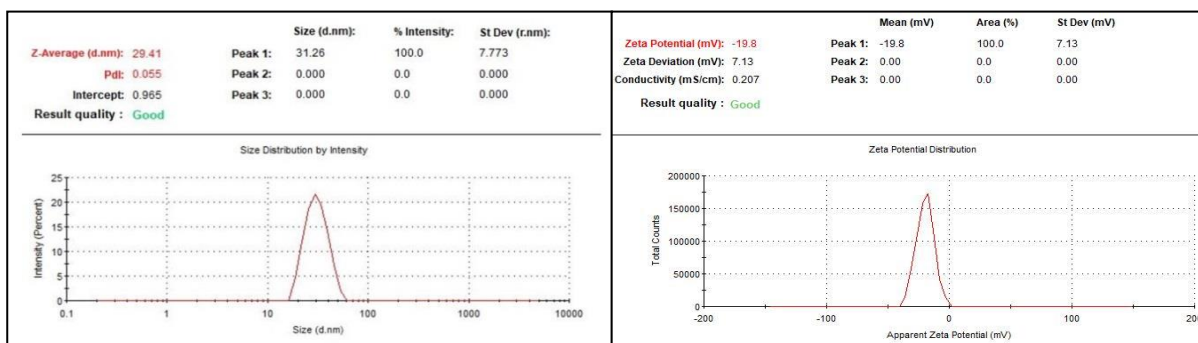
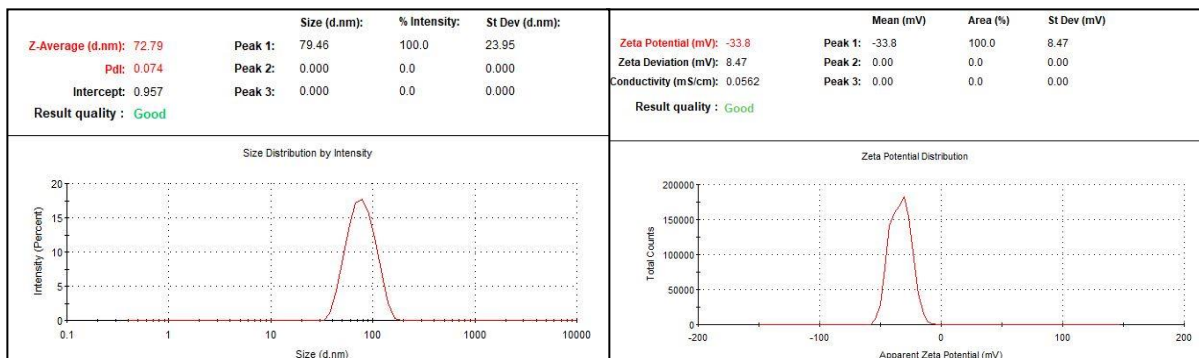


Figure 4. Size (a) and charge (b) of SPION@DEX-BLN-FA using dynamic light scattering (DLS).

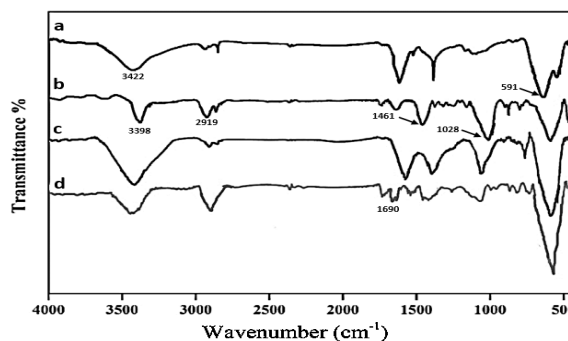


3.1.3. FT-IR spectral analysis

The addition of different coatings on SPIONs was verified by the use of FTIR spectrum analysis. The characteristic peaks of the SPIONs, both coated and uncoated were depicted in Figure 6. A The distinctive band at 591 cm⁻¹ is correspond to the vibration of Fe-O for all the samples. The peak of absorption at 3422 cm⁻¹ was represent the bare SPIONs (Fig. 6 a) that corresponds to the stretching vibration of OH was shows that the iron oxide particles' surface has a lot of hydroxyl groups; which in turn increases the proclivity of the produced SPIONs to aggregate. (19,20) Moreover, the C-H bond's vibrational bending causes a peak at 1461 cm⁻¹ in the DEX- SPIONs molecule's FTIR spectrum, while the stretching vibration of -CH₂- groups was reflected by a peak at 2919 cm⁻¹. While an absorption line at 1028 cm⁻¹ and a signal at 3398 cm⁻¹ due to the stretching vibration of the etheric bond (C-O), and alcoholic group respectively. (Figure. 6b) (21). Although though the main section of the spectra are overlapped, the distinctive peaks of BLN in SPION-DEX-BLN can be identified by comparing spectra b and c. In other words, it proved beyond a doubt that SPION-DEX and BLN were successfully captured. Due to SPION-DEX-functionalization BLN's with folate, the SPION-DEX-BLN-FA spectra had a peak at 1690 cm⁻¹ that was associated with

the carboxyl group of folic acid, confirming the existence of this molecule.

Figure 5. FT-IR spectra a, b, c, and d belong to SPION, DEX-SPPION, BLN-DEX-SPION, and FA-BLN-DEX-SPION respectively.

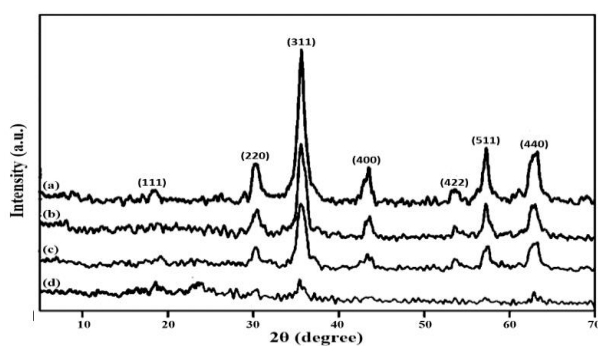


3.1.4. X-ray diffraction patterns (XRD)

The XRD patterns of the SPION, SPION-DEX, SPION-DEX-BLN, and SPION-DEX-BLN-FA are shown in Figure 7. Several peaks at $2\theta = 17.95^\circ$ (111), 29.80° (220), 36.03° (311), 44.10° (400), 54.21° (422), 56.93° (511) and 62.71° (440) were detected for the naked SPIONs and are indexed as those of the inverse spinal structure of magnetite (JCPDS card No. 01-088-0866) (Fig. 7a). The absence of other forms of iron oxides in the produced product is also indicated by the XRD examination. The results of the XRD examination also show that the synthesized product lacks the other forms of iron oxides (22). It was important to understand that for

the SPION-DEX and SPION-DEX-BLN, the typical peaks remained visible and did not vanish, although their peak intensities and widths changed due to diffraction. (Figure. 7b, c). Whereas in the case of SPION-DEX-BLN-FA peaks almost disappeared may be due to of polymer amorphous properties and bilayer coverage (Figure. 7d).

Figure 6. XRD spectra of SPION (a) SPION-DEX (b) SPION-DEX-BLN (c) SPION-DEX- BLN-FA (d).



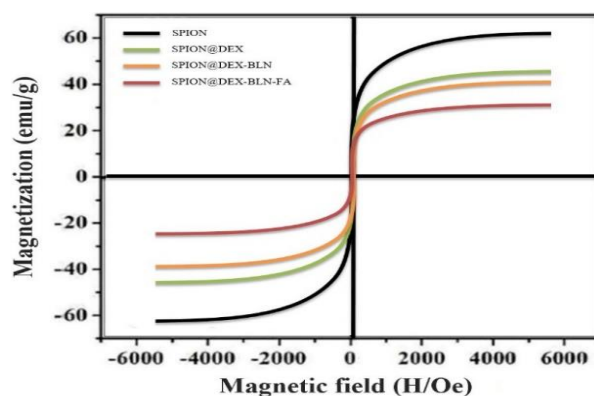
3.1.5. Vibrating sample magnetometry (VSM)

As demonstrated in unmodified formula of SPION, Fe₃O₄-DEX, Fe₃O₄-DEX-BLN, and Fe₃O₄-DEX-BLN-FA, VSM, was utilized to determine the magnetic characteristics of nanoparticles. DEX-coated SPION had a VSM of 44 emu/g, whereas the DEX-SPION included BLN and bleomycin with FA-DEX-SPION had VSMs of 39 and 30, respectively. The unmodified SPION had a VSM of 61 emu/g. (Figure. 8). This drop in saturation magnetization was caused by the nanoformulation's significant inclusion of diamagnetic dextran. (23).

$$\text{Encapsulation Efficiency (\%)} = \frac{(\text{Total quantity of drug} - \text{Free quantity of drug})}{\text{Total amount of drug}} \times 100 \quad \text{Eq. (1)}$$

$$\text{Encapsulation Efficiency (\%)} = \frac{(1 \text{ mg} - 0.22 \text{ mg})}{1 \text{ mg}} \times 100 = 78\%$$

Figure 7. The Magnetization curve loop of SPION, Fe₃O₄@DEX, Fe₃O₄@DEX-BLN, Fe₃O₄@DEX-BLN-FA at 300 K



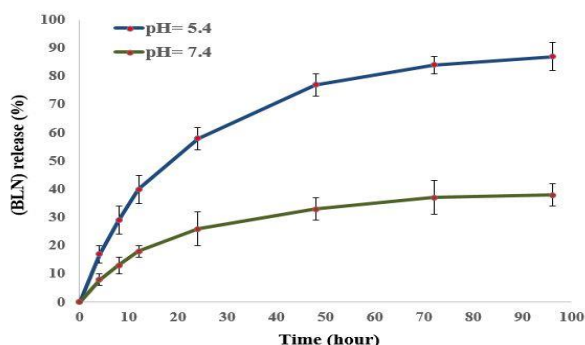
3.2. Encapsulation efficiency of SPION-DEX-BLN-FA

A UV-Vis spectrophotometer at a wavelength of 425 nm was used to estimate the concentration in the supernatant in order to calculate the final BLN including supernatant quantity. The following Equation (1) was used to determine the effectiveness of medication encapsulation. At this point, the nanocomposite demonstrated great stability and suitable drug conservation.

3.3. Release Profile

According to the results in vitro release curves showed (figure 9), BLN releases time from loaded SPION@DEX-BLN-FA nanosystem over a 96-hour period, moreover, the release rate was greater in the citrate buffer with an acidity (pH 5.4) than in phosphate buffer with a neutral (pH 7.4) under the same circumstances. Hence, during 96 hours, 86% of the medication was released in pH 5.4 as opposed to 34% in pH 7.4. Al-Musawi et al., however, used magnetic iron oxide nanoparticles (NPs) coated in chitosan to achieve the similar outcome concerning the curcumin release profile. [25]. In potential hydrogen (pH=7.4) at various temperatures, Eynali et al. in 2017 demonstrated equivalent cumulative in vitro release patterns of BLN from the polymeric coated iron oxide core. (23).

Figure 8. Depicts the FA-DEX-BLN-SPION Nano-in vitro release profile at pH 7.4 and pH 5.4. At 37 °C, all trials were conducted. Data are mean values with standard deviations (n = 3).

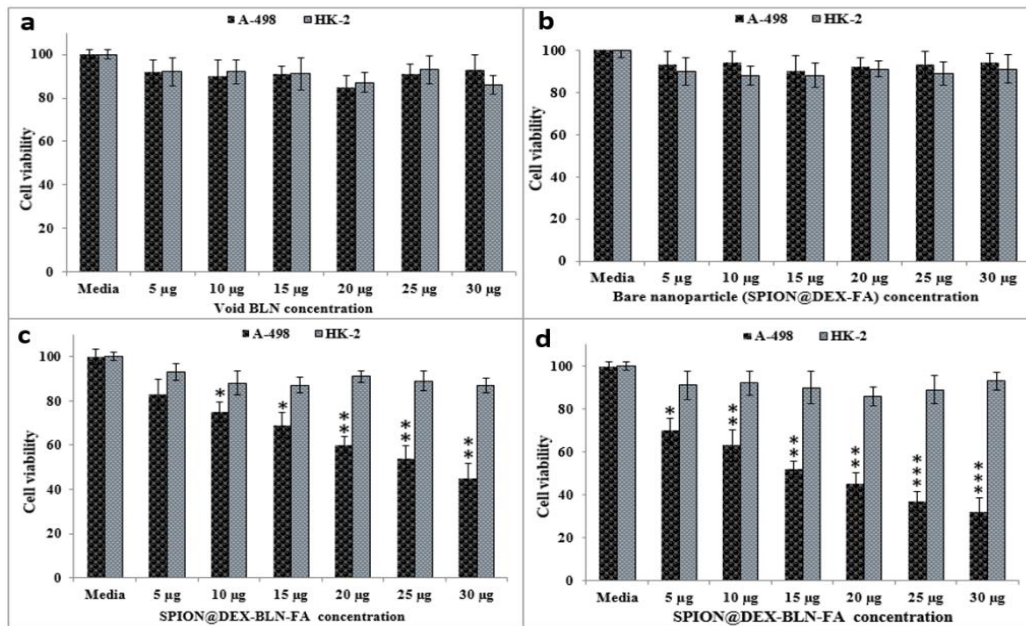


3.4. Methyl thiazolyl tetrazolium (MTT) assay

To complete the MTT, 200 μ l of media containing 1×10^4 cells was added to each well

of cell plate.. For 24 hours, the cells proliferated and stuck to the surface. Each well's medium was taken out and replaced with a brand-new one that contained different concentrations (5 μ g to 30 μ g) of BLN, SPION-DEX-BLN-FA, or SPION-DEX-FA. We looked examined the incubation times of 24 and 48 hours. The control group of cells received no treatment at all. The MTT solution was diluted to the appropriate strength (each 100 μ l of media contained ten milliliter (10 μ l) of the five(5) mg/ml solution) and poured into every well and incubation of the plates for four hours at 37 °C in a humidified environment that was composed of 95% air and 5% CO₂. To dissolve the formazan crystals, 100 μ l of DMSO was injected to each well after the residual MTT solution was drained. To guarantee that the formazan crystals were sufficiently dissolved, the plates were shaken for five minutes. Using a multi-scan plate reader, the absorbance of each well was measured at 540 nm (VERSAmax microplate reader, Molecular Device, CA, USA). In order to get the results, mean and SD were used. According to the results of the study's IC₅₀, the concentrations for 24 and 48 hours were 28 μ g and 19 μ g, respectively (Figure. 11). The current findings showed that DEX, SPION, and FA targeted nanoparticles were more potent to improve effectiveness and efficiency of BLN. The IC₅₀ of BLN loaded polyethylene glycol coated magnetic layered double hydroxide (PEG-FU-MLDH) against HepG2 liver cancer cells was determined to be 28.88 μ g/mL. (15). The current findings indicated that FA targeted, DEX, and SPION NPs were more potent to improve effectiveness and efficiency of BLN.

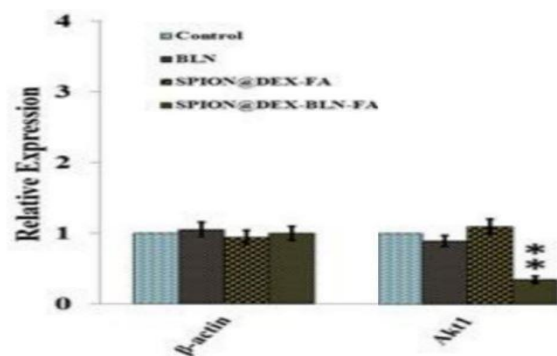
Figure 9. Cytotoxic effect of various concentrations (5–30 μg) of a) void BLN drug and b) bare nanoparticles (SPION@DEX-FA) after 48 h and SPION@DEX-BLN-FA at c) 24 h and d) 48 h on A-498 cancer and HK-2 normal cell lines (mean \pm S.D., (* $p < 0.05$; ** $p < 0.01$; *** $p < 0.001$); $n = 3$).



3.7. Gene Expression

qPCR was used to analyze the expression levels of the AKT1 gene, in addition to using beta-actin as a reference control gene (housekeeping gene). Figure 12 illustrates the considerable variation in AKT1 gene expression between cancerous and non-cancerous tissues. Both with and without BLN therapy, expression levels of beta-actin in control and malignant cells remain unchanged. However, gene expression levels of the AKT1 clearly rose when malignant cells were treated with FA-DEX-BLN-SPION as compared/apposite to void BLN and SPION-DEX-FA (**** $P < 0.0001$).

Figure 10. Figure 12 shows the results of a two-way ANOVA and Bonferroni post-test on a real-time PCR gene expression analysis of A-498 cancer cells treated with void BLN, SPION@DEX-BLN-FA, and SPION@DEX-FA. The graph's values show the mean and standard deviation. Significant differences between the control (untreated) and other treatments are indicated by ** $p < 0.01$ and *** $p < 0.001$.



4. Discussion

The co-precipitation method was effectively used to development of dextran-coated superparamagnetic nanoparticles (DEX-SPION), which transported BLN; the Nano-carrier supported the drug loading with nanoscale particle size distribution.. Microscopic examination revealed that the NPs were smooth, sphere-shaped, and free of stickiness, which was completely consistent with other observations (18). Concerning FT-IR spectral analysis although though the main section of the spectra are overlapped, the distinctive peaks of BLN in SPION-DEX-BLN can be identified by comparing spectra b and c. In other words, it proved beyond a doubt that SPION-DEX and BLN were successfully captured. Due to SPION-DEX-functionalization BLN's with folate, the SPION-DEX-BLN-FA spectra had a peak at 1690 cm⁻¹ that was associated with the carboxyl group of folic acid, confirming the existence of this molecule.

Al-Musawi et al., however, used magnetic iron oxide nanoparticles (NPs) coated in chitosan to achieve the same outcome regarding the curcumin release profile. (24). Eynali et al. demonstrated that the accumulative in vitro release patterns of BLN from the DEX-FA-SPION in pH=7.4 at various temperatures were identical (25). According to the findings, SPION-DEX-BLN-FA is a reliable co-delivery method for BLN. Nanoparticles called SPION-DEX-BLN-FA have a sustained release profile, which leading to dose and time dependent targeted kidney cell cytotoxicity. SPION-DEX-BLN-FA has an inhibiting activity against tumor growth in the renal cancer more markedly than BLN alone and SPION-DEX-FA. The SPION-DEX-BLN-FA also exhibits great controllability, loading efficiency, biocompatibility, and penetrability, making it a valuable drug delivery system and intriguing tool for a variety of possible biomedical applications (24,25). In

comparison to void BLN and SPION-DEX-FA, it is suggested that SPION-DEX-BLN-FA could cause cytotoxic effects on Akt1 gene expression level, a decrease in malignant cells, and successfully limit the progression without harm to healthy cells. As a result, it might be used as a reliable and effective anti-tumor factor with potential for therapeutic use.

Reference

- Ales Groselj, Masa Bosnjak, Mojca Krzan, Tina Kosjek, Kriszta Bottyán,8 Helena Plesnik, Crt Jamsek, Maja Cemazar, Erika Kis, and Gregor Sersa. Bleomycin Concentration in Patients' Plasma and Tumors after Electrochemotherapy. A Study from InspECT Group. *Pharmaceutics*. 2021 Sep; 13(9): 1324.
- Freeman-Cook KD, Autry C, Borzillo G, Gordon D, Barbacci-Tobin E, Bernardo V, et al. (June 2010). "Design of selective, ATP-competitive inhibitors of Akt". *Journal of Medicinal Chemistry*. 53 (12): 4615–22.
- Camillo Porta, Chiara Paglino, Alessandra Mosca. Targeting PI3K/Akt/mTOR Signaling in Cancer. *Front Oncol*. 2014; 4: 64.
- Kumar A, Purohit R. Cancer associated E17K mutation causes rapid conformational drift in AKT1 Pleckstrin Homology (PH) Domain. *PLoS ONE*. 2013;8(5)e64364.
- Heerding DA, Rhodes N, Leber JD, Clark TJ, Keenan RM, Lafrance LV, et al. (September 2008). "Identification of 4-(2-(4-amino-1,2,5-oxadiazol-3-yl)-1-ethyl-7-((3S)-3-piperidinylmethyl)oxy)-1H-imidazo[4,5-c]pyridin-4-yl)-2-methyl-3-butyn-2-ol (GSK690693), a novel inhibitor of AKT kinase". *Journal of Medicinal Chemistry*. 51 (18): 5663–79.
- Chen WS, Xu PZ, Gottlob K, Chen ML, Sokol K, Shiyanova T, et al. (September

- 2001). "Growth retardation and increased apoptosis in mice with homozygous disruption of the Akt1 gene". *Genes & Development*. 15 (17): 2203–8.
- Staal SP, Hartley JW, Rowe WP (July 1977). "Isolation of transforming murine leukemia viruses from mice with a high incidence of spontaneous lymphoma". *Proceedings of the National Academy of Sciences of the United States of America*. 74 (7): 3065–7.
- Song G, Ouyang G, Bao S (2005). "The activation of Akt/PKB signaling pathway and cell survival". *Journal of Cellular and Molecular Medicine*. 9 (1): 59–71
- Alberts B, Johnson A, Lewis J, Raff M, Roberts K, Walter P (2002). "Figure 15-60: BAD phosphorylation by Akt". *Molecular biology of the cell*. New York: Garland Science. ISBN 978-0-8153-3218-3.
- Dadfar SM, Roemhild K, Drude NI, von Stillfried S, Knüchel R, Kiessling F, Lammers T. Iron oxide nanoparticles: diagnostic, therapeutic and theranostic applications. *Adv Drug Deliv Rev*. 2019;138:302–25.
- Gupta AK, Gupta M. Synthesis and surface engineering of iron oxide nanoparticles for biomedical applications. *Biomaterials*. 2005;26:3995–4021.
- Al-Musawi, S.; Kadhim, M.J.; Hindi, N.K.K. Folated-nanocarrier for paclitaxel drug delivery in leukemia cancer therapy. *J. Pharm. Sci. Res*. 2018, 10, 749–754.
- Albukhaty, Sharafaldin Al-Musawi, Salih Abdul Mahdi, Ghassan M. Sulaiman, Mona S. Alwahibi, Yaser Hassan Dewir, Dina A. Soliman, and Humaira Rizwana. Investigation of Dextran-Coated Superparamagnetic Nanoparticles for Targeted Vinblastine Controlled Release, Delivery, Apoptosis Induction, and Gen Expression in Pancreatic Cancer Cells. *Molecules* 2020, 25, 4721.
- Lévy R, Thanh NTK, Doty RC, et al. Rational and combinatorial design of peptide capping ligands for gold nanoparticles. *J Am Chem Soc*. 2004;126(32):10076–10084.
- M. Ebadi, B. Saifullah, K. Buskaran, et al. Synthesis and properties of magnetic nanotheranostics coated with polyethylene glycol/5-fluorouracil/layered double hydroxide *Int J Nanomed*, 14 (2019), pp. 6661-6678.
- Sharafaldin Al-Musawi, Sumayah Ibraheem, Salih Abdul Mahdi, Salim Albukhaty, Adawiya J. Haider, Afraa Ali Kadhim, Kadhim Ali Kadhim, Haitham Ali Kadhim, and Hassan Al-Karagoly. Smart Nanoformulation Based on Polymeric Magnetic Nanoparticles and Vincristine Drug: A Novel Therapy for Apoptotic Gene Expression in Tumors. *Life* 2021, 11(1), 71.
- Sharafaldin Al-Musawi, Salim Albukhaty, Hassan Al-Karagoly, and Faizah Almalki. Design and Synthesis of Multi-Functional Superparamagnetic Core-Gold Shell Nanoparticles Coated with Chitosan and Folate for Targeted Antitumor Therapy. *Nanomaterials (Basel)*. 2021 Jan; 11(1): 32.
- Manjili, H.K., et al., The effect of iron-gold core shell magnetic nanoparticles on the sensitization of breast cancer cells to irradiation. *Archives of Advances in Biosciences*, 2014. 5(2).
- Ahmad S, Riaz U, Kaushik A. Soft template synthesis of super paramagnetic Fe₃O₄ nanoparticles a novel technique. *J Inorg Organomet Polymer Mater*. 2009;19:355–60.

- Sadighian S, Rostamizadeh K, Hosseini-Monfareda H, Hamidi M. Doxorubicin-conjugated core-shell magnetite nanoparticles as dual-targeting carriers for anticancer drug delivery. *Colloids Surf B Biointerfaces*. 2014;117:406–13.
- Bai H, Liu Z, Delai SD. Highly water soluble and recovered dextran coated Fe₃O₄ magnetic nanoparticles for brackish water desalination. *Sep Purif Technol*. 2011;81:392–9.
- Petcharoen K, Sirivat A. Synthesis and characterization of magnetite nanoparticles via the chemical coprecipitation method. *Mater Sci Eng B*. 2012;177:421–7.
- Zhu, Y.; Yang, L.; Huang, D.; Zhu, Q. Molecularly imprinted nanoparticles and their releasing properties, bio-distribution as drug carriers. *Asian J. Pharm. Sci*. 2017, 12, 172–178
- Al-Musawi, S., et al., Preparation and Characterization of Folate-Targeted Chitosan/Magnetic Nanocarrier for 5-Fluorouracil Drug Delivery and Studying its Effect in Bladder Cancer Therapy. 2009.
- Eynali, S., et al., Evaluation of the cytotoxic effects of hyperthermia and 5-fluorouracil-loaded magnetic nanoparticles on human colon cancer cell line HT-29. *International Journal of Hyperthermia*, 2017. 33(3): p. 327-335.